Growth of epitaxial $NdNiO_3$ and integration with Si(100)

Ashutosh Tiwari,[a] J. Narayan, C. Jin, and A. Kvit
Department of Materials Science and Engineering, North Carolina State University, Raleigh, North Carolina 27695-7916

(Received 14 September 2001; accepted for publication 12 December 2001)

We have grown epitaxial $NdNiO_3$ films on Si(100) substrate under ambient oxygen pressure using a pulsed-laser deposition method. The integration of $NdNiO_3$ with Si(100) was accomplished by lattice-matching epitaxy of MgO and $SrTiO_3$ and domain matching epitaxy of TiN on Si(100). During domain matching epitaxy, four lattice constants of TiN match with three of silicon across the TiN/Si(100) interface. High-quality epitaxial $NdNiO_3$ film on $SrTiO_3$/MgO/TiN/Si(100) showed a very sharp metal–insulator (MI) phase transition at 200 K. Observed MI transition in epitaxial $NdNiO_3$ is much sharper than that usually observed in bulk and polycrystalline films with more than four orders of magnitude change in resistivity. This MI transition is understood to arise because of the opening of charge transfer gap between $Ni^{3+}(3d)$ and $O^{2-}(2p)$ band. © *2002 American Institute of Physics.* [DOI: 10.1063/1.1451984]

During the last decade there has been considerable interest in the study of nickelates of the type $RENiO_3$ (RE: rare earth).[1–4] These oxides have been known for a long time[5] but after the discovery of high temperature superconductivity and giant magnetoresistance (GMR) in similarly structured oxides gained a renewed interest. The first member of the series ($LaNiO_3$)[6] is a metal while the other members (RE: Pr, Nd, etc.) are either insulators or undergo a metal–insulator (MI) transition as a function of temperature. The presence of a sharp (MI) transition as a function of temperature makes these materials very important for their potential applications such as bolometers, temperature modulated switches, or optical switches.

For any actual technological application it is essential to deposit thin films of these materials. In the past, efforts[7,8] have been made to deposit thin films of these oxides on variety of substrates like $LaAlO_3$, MgO, $SrTiO_3$, and $NdGaO_3$ using various deposition tecniques. These films were found to be epitaxial on $LaAlO_3$(100) and textured on other substrates.[7,8] The integration of $NdNiO_3$ on Si(100) presents additional challenging problems. The growth of $NdNiO_3$ films on silicon is very difficult due to large lattice mismatch and high diffusivity of its constituents into silicon at typical deposition temperatures $\sim 600-700\,^\circ C$.

Recently, we have grown epitaxial $NdNiO_3$ films on Si(100) substrates by using a multilayered thin buffer layer. This buffer layer consists of TiN, MgO, and $SrTiO_3$. TiN was chosen because of its diffusion barrier properties and it grows epitaxialy on Si(100). Three lattice constants of Si match very well with four of TiN and the epitaxial growth occurs via domain matching epitaxy.[9] TiN has excellent lattice match with MgO, which has quite good lattice match with $SrTiO_3$. Lattice constant of $SrTiO_3$ matches with that of $NdNiO_3$ within 2.5%. This unique selection of buffer layers made it possible to integrate epitaxial thin film of $NdNiO_3$ on Si(100) with excellent switching characteristics. The availability of thin films of rare-earth nickelates on silicon chips is likely to open a cascade of opportunities for perovskite based microelectronics.

Thin film deposition was performed in a multitarget pulsed laser deposition chamber with a KrF excimer laser (Lambda Physik 210, $\lambda = 248$ nm). TiN, MgO, $SrTiO_3$, and $NdNiO_3$ targets were ablated sequentially in the same run. The deposition of TiN film was done at $600\,^\circ C$ in vacuum (2×10^{-7} Torr). After TiN, MgO was deposited for 10 min at the same temperature in the oxygen pressure of 2×10^{-5} Torr. For $SrTiO_3$ deposition substrate temperature was raised to $700\,^\circ C$ and oxygen pressure to 1×10^{-3} Torr. For $NdNiO_3$ deposition substrate temperature was $650\,^\circ C$ and oxygen pressure was 1×10^{-1} Torr. The energy density and pulse frequency were 1.5–3 J/cm^2 and 10 Hz, respectively. $NdNiO_3$ target used for ablation was prepared by a solgel method described somewhere else.[10] In this approach stoichiometric amounts of Nd_2O_3, $Ni(NO_3)_2\cdot 6H_2O$ were dissolved in nitric acid and citric acid was added to this solution so as to maintain the ratio of Nd:Ni:citric acid as 1:1:2.05. The molarity of this solution was maintained at 0.1 M and the solution was refluxed at $90\,^\circ C$ for 24 h. The solution was gently evaporated to get a fluffy gel which was fired at $650\,^\circ C$ for 12 h. The powder sample was pressed in the form of circular pellet and sintered at $750\,^\circ C$ for seven days in flowing oxygen. $NdNiO_3$ film was characterized using x-ray diffraction (Cu $K\alpha$ radiation) and transmission electron microscope. Precise measurement of electrical resistivity was done in the temperature range 20–300 K.

X-ray diffraction pattern of $NdNiO_3$/$SrTiO_3$/MgO/TiN multilayer structure on Si(100) substrate is shown in Fig. 1. It is evident from this pattern that all the layers show preferential orientation (100) parallel to substrate, suggesting the epitaxial growth of the multilayered structure. In the 2θ range of 20–80 we could see only (100) and (200) lines of $NdNiO_3$ and $SrTiO_3$ and (200) line for MgO and TiN films in addition to a sharp peak for (400) plane of Si. From the XRD data we determined the in-plane lattice parameter to be 3.812

[a]Electronic mail: atiwari@unity.ncsu.edu

 © 2002 American Institute of Physics
Downloaded 12 Feb 2010 to 155.97.11.183. Redistribution subject to AIP license or copyright; see http://apl.aip.org/apl/copyright.jsp

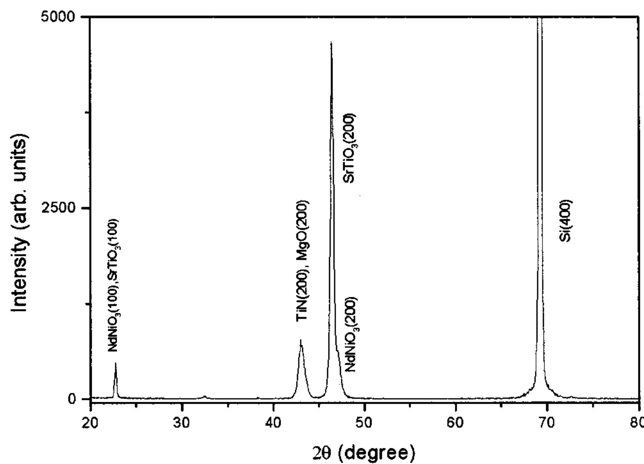

FIG. 1. X-ray diffraction pattern of epitaxial $NdNiO_3$ on Si(100) substrate with TiN, MgO, and $SrTiO_3$ as buffer layers.

Å which is quite close to pseudocubic lattice parameter $a_{\mathrm{pseudo}} = 3.807$ Å for bulk sample.[11]

Figure 2(a) shows a cross-sectional TEM image of $NdNiO_3/SrTiO_3$/MgO/TiN/Si(100) layers along ⟨011⟩ direction of silicon substrate. The growth of uniform layers of TiN, MgO, $SrTiO_3$, and $NdNiO_3$ on silicon substrate is clearly shown in the figure. A high resolution TEM micrograph in Fig. 2(b) establishes the epitaxial growth of $NdNiO_3$ on $SrTiO_3$, where the interface between $NdNiO_3$ and $SrTiO_3$ is atomically sharp with no evidence of significant interdiffusion. Figure 2(c) shows a Fourier transform diffraction pattern from the region indicated in Fig. 2(b). This pattern contains diffraction spots corresponding to ⟨011⟩ orientation with cube-on-cube epitaxial relationship with $SrTiO_3$.

Electrical resistivity versus temperature for epitaxial $NdNiO_3$ is shown in Fig. 3. This figure shows that $NdNiO_3$ film undergoes a very sharp MI transition at about ~200 K. Above 200 K it behaves as a metal and below it as an insulator. More than four orders of magnitude change in electrical resistivity is observed across the transition. Room temperature resistivity of the film was 1.2 mΩ cm. Quite similar to high-oxygen-pressure prepared bulk and polycrystalline films,[3,8] the electrical resistivity of epitaxial $NdNiO_3$ also showed a thermal hysteresis in the temperature range 105–200 K. This confirms that the thermal hysteresis in resistivity is an intrinsic property of the system and manifests the first order nature of the MI transition. In a first order phase transition, over a certain range of temperature close to MI transition, high temperature metallic, and low temperature insulating phase may coexist giving rise to an hysteretic behavior in the electrical transport.

In insulating transition metal oxides the temperature dependence of electrical resistivity is usually governed either by the activated conduction mechanism ($\log \rho \propto 1/T$) or by the variable range hopping conduction mechanism ($\log \rho \propto 1/T^{1/4}$). We fitted our resistivity data to the expressions corresponding to both of these mechanisms. Figure 4 shows the plots of $\log_{10}(\rho)$ vs $1/T$ and $1/T^{1/4}$. It is clear from this figure that both the curves deviate from straight line behavior, ruling out the possibility of any of these mechanisms solely determining the conduction in the insulating phase of $NdNiO_3$. It is interesting to see that in Fig. 4(a) the $\log_{10}(\rho)$

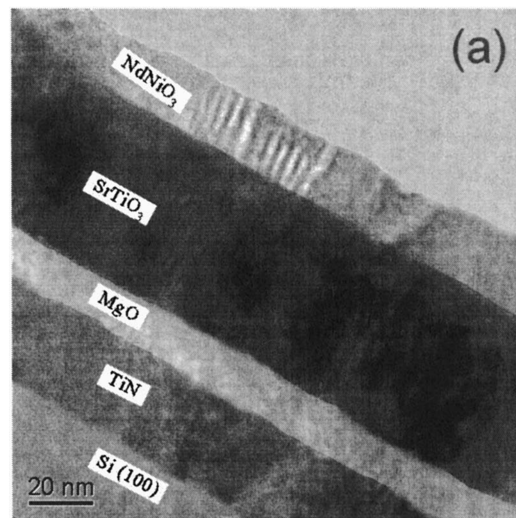

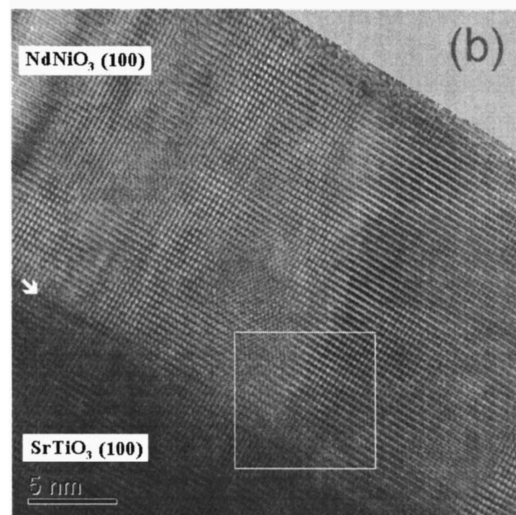

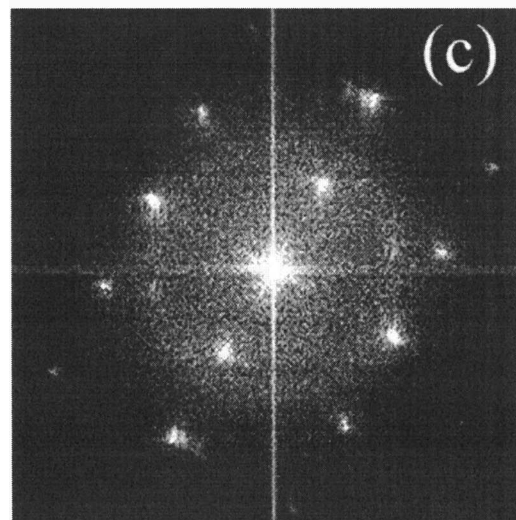

FIG. 2. (a) Cross-sectional image of $NdNiO_3/SrTiO_3$/MgO/TiN/Si(100) structure along ⟨011⟩ direction; (b) high resolution TEM image of $SrTiO_3$ and $NdNiO_3$; (c) Fourier transform diffraction pattern from the region indicated in (b).

vs $1/T$ shows a smooth upward curvature. Using the local slopes of this curve and the resistivity expression for activated conduction $[\rho(T) = \rho_0 \exp(E_g/kT)]$, we estimated the values of activation band gap, E_g, to be 4 meV at 100 K and 11 meV at 20 K. This increase in the insulating band gap at

Downloaded 12 Feb 2010 to 155.97.11.183. Redistribution subject to AIP license or copyright; see http://apl.aip.org/apl/copyright.jsp

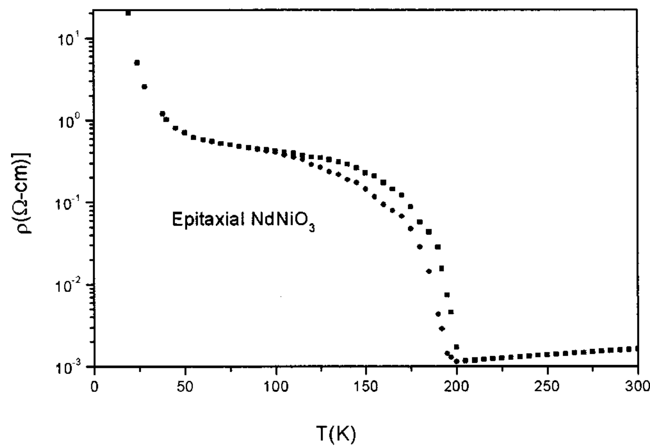

FIG. 3. Electrical resistivity of epitaxial $NdNiO_3$ film. Lower curve is for cooling cycle while upper curve is for the heating cycle.

lower temperatures is in good agreement with the ZSA model[12] proposed by Zaanen, Sawatzky, and Allen to explain the behavior of transition metal compounds. According to this model there is a charge transfer gap between occupied O^{2-} $2P$ valence band and the unoccupied Ni^{3+} $3d$ conduction band. The Fermi level resides in this gap and hence the material is insulating. When temperature increases because of the thermal broadening the bandwidth also increases. As a consequence of the increase in bandwidth, the charge transfer gap decreases eventually becoming zero as the valence band and conduction band overlap, giving rise to a metallic state.[12]

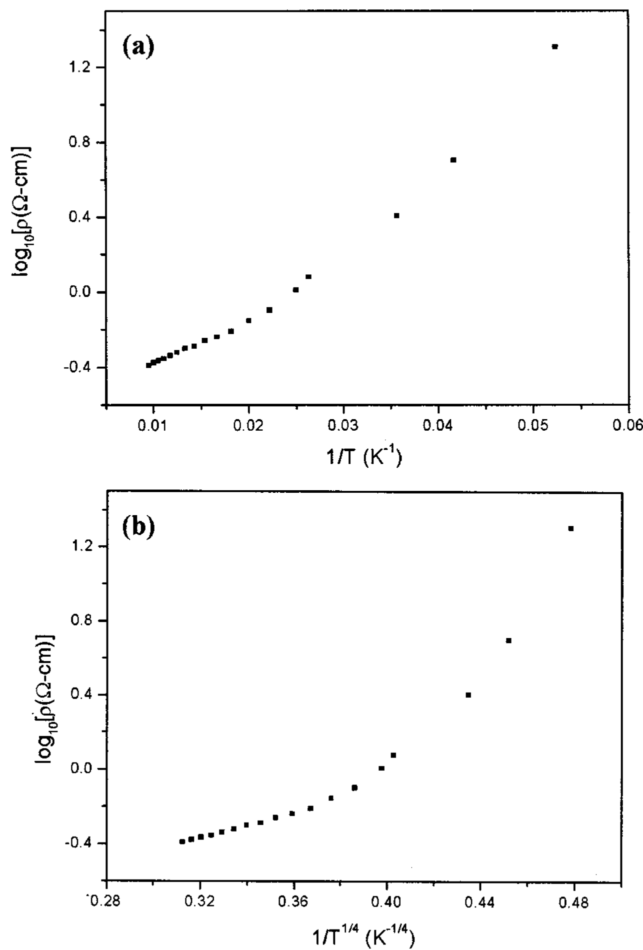

FIG. 4. (a) $\log_{10}(\rho)$ vs $1/T$; (b) $\log_{10}(\rho)$ vs $1/T^{1/4}$. In both cases a deviation from the straight line behavior can easily be envisaged.

At this point we find it appropriate to mention that it is extremely difficult to stabilize Ni^{3+} under the normal conditions of temperature and pressure. To achieve it the annealing of the sample at high temperature and high oxygen pressure is required.[3,13] But in our experiment epitaxial growth of $NdNiO_3$ occurred under ambient oxygen pressure without any need for further annealing of the film. This became possible because of the high energy of plume involved in the pulsed laser deposition.[14] Ionized species in plume have energies of the order of several hundreds of eV which is much higher than the ionization potential of Ni^{3+} (~ 35 eV). In order to dilute the lattice mismatch between $NdNiO_3$ and Si, intermediate layers of TiN, MgO, and $SrTiO_3$ were used. We also tried to deposit $NdNiO_3$ on Si(100) directly and also by using only TiN and MgO buffer layers. Film on Si(100) was found to be polycrystalline with some NiO impurities while the film with TiN/MgO buffer layer was textured having some minor NiO impurities. In both of the above cases film showed much inferior switching characteristic than that observed in epitaxial $NdNiO_3$.

Finally we conclude this letter by stating that we have integrated $NdNiO_3$ film on silicon chip using a pulsed laser deposition techique. Fabrication of thin $NdNiO_3$ film with sharp MI transition on silicon is likely to open numerous opportunities for perovskite based microelectronics.

[1] X. Q. Xu, J. L. Peng, Z. Y. Li, H. L. Ju, and R. L. Greene, Phys. Rev. B **48**, 1112 (1993).
[2] P. C. Canfield, J. D. Thompson, S.-W. Cheong, and L. W. Rupp, Phys. Rev. B **47**, 12357 (1993).
[3] J. B. Torrance, P. Lacorre, A. I. Nazzal, E. J. Ansaldo, and Ch. Niedermayer, Phys. Rev. B **45**, 8209 (1992).
[4] X. Granados, J. Fontcuberta, X. Obradors, Ll. Mañosa, and J. B. Torrance, Phys. Rev. B **48**, 11666 (1993).
[5] G. Demazeau, A. Marbeuf, M. Pouchard, and P. Hagenmuller, J. Solid State Chem. **3**, 582 (1971).
[6] A. Tiwari and K. P. Rajeev, J. Phys.: Condens. Matter **11**, 3291 (1999).
[7] M. A. Novojilov, O. Yu. Gorbenko, I. E. Grayboy, A. R. Kaul, H. W. Zandbergen, N. A. Babushkina, and L. M. Belova, Appl. Phys. Lett. **67**, 557 (1995).
[8] G. Catalan, R. M. Bowman, and J. M. Gregg, J. Appl. Phys. **87**, 606 (2000).
[9] J. Narayan, P. Tiwari, X. Chen, J. Singh, R. Chowdhury, and T. Zheleva, Appl. Phys. Lett. **61**, 1290 (1992); J. Narayan, U.S. Patent No. 5, 406, 123 (April 11, 1995).
[10] A. Tiwari and K. P. Rajeev, Solid State Commun. **109**, 119 (1999).
[11] P. Lacorre, J. B. Torrance, J. Pannetier, A. I. Nazzal, P. Wang, and T. C. Huang, J. Solid State Chem. **91**, 225 (1991).
[12] J. Zaanen, G. A. Sawatzky, and J. W. Allen, Phys. Rev. Lett. **55**, 418 (1985).
[13] J. F. DeNatale and P. H. Kobrin, J. Mater. Res. **10**, 2992 (1995).
[14] R. K. Singh and J. Narayan, Phys. Rev. B **41**, 8843 (1990).